ROBOTIC ASSISTANCE FOR CHILDREN WITH CEREBRAL PALSY BASED ON LEARNING FROM TELE-COOPERATIIVE DEMONSTRATION

Mohammad Najafi [*]*, Mojtaba sharifi, Kim Adams, Mahdi Tavakoli*

ABSTRACT

Physical interaction with environment and object manipulation play an important role in development of children's cognitive and perceptual skills. For children who have severe physical impairments, one of the biggest concerns is the loss of opportunities for meaningful play. Assistive robots can enable children to engage in play activities. In this paper, we focus on robotic assistance for position-following play activities such as pick and place. This task is done via a master-slave teleoperation system with the master robot in the child's hand and the slave robot performing the task in the environment. In the demonstration phase, a therapist (or, in general, a helper such as a parent) holds the slave robot in the task environment to modify and assist the child's movements as the child controls the master robot. A Learning from Demonstration (LfD) technique, which utilizes Gaussian mixture models (GMM) and Gaussian Mixture regression (GMR), is used to learn the helper-administered assistance to the child for completing the task. These probabilistic models provide insight into how the helper assisted the child by analyzing the multiple trials of demonstration in the presence of the helper. In the robotic assistance phase, the robot will utilize the learned data to assist the child in the helper's absence and on a child-specific and as-needed basis. The efficacy of this framework is validated through experimental conducted involving a 2D play environment.

Keywords: Assistive technologies, Teleoperation system, Learning from demonstration, Impedance control

1. INTRODUCTION

Cerebral palsy (CP) is a group of non-progressive disorders in the central nervous system (CNS) that causes permanent posture and movement impairments in children within the first few years of their life [1, 2]. The most common symptoms of CP are poor coordination in performing a voluntary movement, weakness, stiffness of muscles, tremor, delay in acquiring motor skills and difficulty in speaking or swallowing. CP is the dominant origin of motor disability in childhood, which affects 1.5 to more than 4 per 1,000 children around the world [3, 4].

Although the CP symptoms are permanent, they may be improved. Physical therapy and occupational therapy can help children with CP to ameliorate their motor function and live more independently by adjusting to their impairment [5]. However, based on a systematic review [6], these therapeutic approaches are only mildly effective to rehabilitate CP symptoms. A more crucial concern for children with severe disability is missing the ability and opportunity to interact with real physical environments for object manipulation or general play[7]. This deprivation can hinder and adversely affect their natural, social, cognitive, perceptual and linguistic development [8]. To address this issue, we are motivated to develop a semi-autonomous robotic-assistance framework that only requires short-term involvements of a "helper" such as a parent or a therapist (called "therapist" from this point on, for brevity). This platform will not only assist the child to achieve meaningful play through robotic interface to regain their natural development, but will also ensure their active physical participation by using an assist-as-needed (AAN) strategy [9].

Providing direct human assistance to patients with disability is very expensive and impractical [10]. Thus, robotic manipulators have been suggested to take on this burden. The robots are appropriate for assistive purposes as they can perform a repetitive task for long durations without getting exhausted or bored. They can also measure valuable sensory data to evaluate the users' performance and learn their unique execution and behavioral characteristic [11]. Robotic devices can also take the form of master-slave teleoperation systems, in which a human user handling the master robot controls the slave robot interacting with a task environment [12]. This can be helpful as children with disability will be empowered to perform tasks beyond their motor capability and/or range of motion by using position and force scaling in the teleoperation system [13].

A teleoperation system can be unilateral (without haptic feedback) or bilateral (with haptic feedback). In the former, the slave follows the position of the master while there is no force feedback from task environment of the slave being sent to the master. In the latter, there is bilateral signal

transmission between the master and slave robots, which provides the human operator with the feeling of the remote environment and an experience of "telepresence" [14]. In the ideal "transparent" condition, the bilateral teleoperation system provides perfect force-position reflection between the master and slave robotic manipulators. Thus, the operator perceives perfect telepresence, as if he/she is directly interacting the task environment [12, 15].

Robotic-assistance with an AAN strategy not only motivate children's active participation in the task, but also provokes motor recovery and physical therapy. Several control frameworks have been suggested for ANN including impedance/admittance control [16], which is most beneficial in applications with human-robot interaction as the robot controller imposes a virtual mass-spring-damper behavior in the interaction dynamic [17, 18]. This provides an adjustable flexibility required for interactive tasks. A virtual impedance model connecting the patients' hand to a moving target along the predefined trajectory was defined in [19, 20]. Thus, the patient will not feel any assistive force unless he/she deviates from the target trajectory. A force tunnel produced by a virtual impedance model that restricts the patient in directions orthogonal to his/her movement direction was developed in [11]. In [10], a time limit was also proposed for patients to finish a task by defining a moving virtual wall that would push and assist the patient in case they were moving slower than expected. The authors in [21] used position, force and impedance control to provide a virtual-tunnel model for guidance in the tangential and virtual-wall-like restriction in the normal directions of the trajectory.

The major drawback of stated assist-as-needed frameworks is the requirement for robot programing by the therapist in order to plan the desired trajectory. Therapists typically do not have the required programming skills. Also, it would be an arduous struggle for them to mathematically model these task-dependent assistance models every time the task changes (e.g., if the locations of object picking and placing change). As a result, a learning from demonstration (LfD) technique was utilized for rehabilitation applications in [22, 23]. In this framework, the therapist demonstrates to the robotic system the required assistance (external force and/or displacement inputs) for task execution by simply performing the task multiple times. Then, by using Gaussian mixture model (GMM) and Gaussian mixture regression (GMR) [24], the robotic system assists the task performance in the therapist's absence. This strategy is useful as it replaces the need for robot programing with hands-on physical demonstrations of the robot role by a human.

In this paper, the goal is to propose a robotic AAN framework for a two-dimensional (2D) position-following pick-and-place task via a teleoperation system. In this framework, for the first time, a tunnel-like T-N impedance/admittance controller is designed together with Learning from Demonstration (LfD) techniques. The proposed scheme with its demonstration and robotic assistance phases is sketched in Fig. 1. In the first phase, the

therapist provides assistance as needed and cooperates with the child to perform the task for few times. In this phase, the therapist assistance is modeled by a GMM and the average trajectory demonstrated by the therapist is approximated using GMR. In the second phase, tangential-normal impedance models are proposed so that the master robot handled by the child assists the child to follow the average demonstrated trajectory in the tangential direction and resists the child's motion in the normal direction. In both of the tangential and normal directions, the level of assistance/resistance can be adjusted by tuning the parameters of the impedance models.
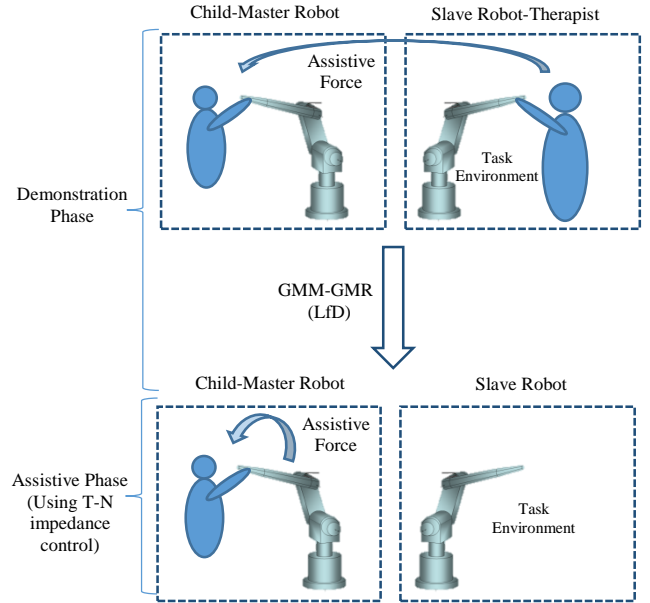
Fig. 1. The schematic of proposed robotic assistance framework including demonstration and assistive phases.

2. DYNAMICS OF MASTER-SLAVE TELEOPERATION SYSTEM

The nonlinear dynamics of the multi-DOF master and slave robots side in the Cartesian coordinates are [25]

$$M_{x,m}(q_m)\ddot{x}_m + C_{x,m}(q_m, \dot{q}_m)\dot{x}_m + G_{x,m}(q_m) + F_{x,m}(\dot{q}_m) = F_m + F_{ext,m} \qquad (1)$$

$$M_{x,s}(q_s)\ddot{x}_s + C_{x,s}(q_s, \dot{q}_s)\dot{x}_s + G_{x,s}(q_s) + F_{x,s}(\dot{q}_s) = F_s + F_{ext,s} \qquad (2)$$

where x_m and $x_s \in R^{n \times 1}$ are, respectively, the positions of the master and slave end-effectors in the Cartesian coordinates. $M_{x,m}(q_s)$ and $M_{x,s}(q_s) \in R^{n \times n}$ are the inertia matrices, $C_{x,m}(q_s, \dot{q}_s)$ and $C_{x,s}(q_s, \dot{q}_s) \in R^{n \times 1}$ contain Coriolis and Centrifugal terms, $G_{x,m}(q_s)$ and $G_{x,s}(q_s)$ vectors represent position-dependent forces such as gravity, $F_{x,m}(\dot{q}_s)$ and $F_{x,s}(\dot{q}_s) \in R^{n \times 1}$ are the friction forces, F_m and $F_s \in R^{n \times 1}$ are the control signals for the robot's actuators and

$F_{ext,m}$ and $F_{ext,s} \in R^{n \times 1}$ are the external forces exerting on robots' end-effector. In this paper, the master and slave robots are respectively in contact with child and the therapist. This means that the external forces are

$$F_{ext,m} = F_{ch} \tag{3}$$

$$F_{ext,s} = -F_{th} - F_e \tag{4}$$

where $F_{ch} \in R^{n \times 1}$ is the child's force exerted on the master robot, and $F_{th} \in R^{n \times 1}$ and $F_e \in R^{n \times 1}$ are, respectively, the therapist's and the task environment's forces applied on the slave robot. Note that as the slave interacts with the task environment, the therapist pulls/pushes the slave in order to assist the child in terms of completing the task. It is assumed that the slave robot is either inherently back-drivable or is properly impedance controlled to follow externally-imposed motions.

3. DEMONSTRATION PHASE

In this paper, a pick and place game is chosen as the position-following task for the child. The child interacting with the master robot manipulates the slave robot to perform the task in the remote environment through a teleoperation system. Meanwhile, the therapist interacts with the slave robot in order to assist and modify the child's movements, considering the child's unique motion and posture characteristics. The position trajectory data from multiple task trials is saved to be encoded using GMM and GMR.

Transparency in the teleoperation system is provided when perfect position and force tracking are simultaneously achieved in the master-slave robotic setup. In order to provide transparency, the Direct Force Reflection (DFR) architecture is employed [11]. In this control method, the master position trajectory is transmitted to and tracked by the slave robot. Also, the slave-therapist interaction force is reflected back to the master robot to be fed back to the child, as schematically shown in Fig. 2.
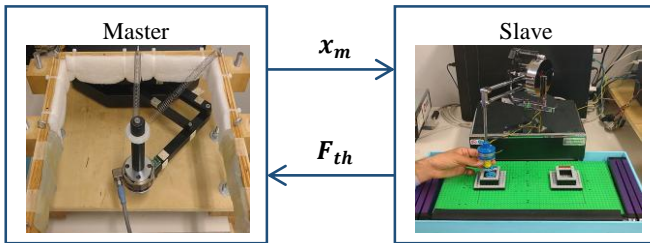
Fig. 2. Direct force reflection (DFR) strategy for the cooperation of the child and therapist in the demonstration phase.

The obtained data from cooperative demonstration of the pick-and-place task through a transparent teleoperation system is constructed by 2-dimensional position vector ($S^P \in R^2$) and a 1-dimensional time variable ($S^t \in R$). The size of the total demonstration dataset is determined by the number of sampled data in each trial (N), multiplied by the total number of demonstration trials (M). So the resulting M.N samples form the total database of

$$\{D = \begin{bmatrix} S_{1,1}^P & S_{1,2}^P & \dots & S_{m,n}^P & \dots & S_{M,N}^P \\ S_{1,1}^t & S_{1,2}^t & \dots & S_{m,n}^t & \dots & S_{M,N}^t \end{bmatrix} \in R^{3 \times M.N} \tag{5}$$
$$: \ \forall \ m \in \{1,2,\dots,M\}, n \in \{1,2,\dots,N\} \ \}$$

In (5), m and n subscripts indicate the nth sample of a signal in the mth demonstration. The Gaussian Mixture Model (GMM) will be used to statistically model the demonstration database ($D \in R^{3 \times M.N}$). The GMM is a probabilistic model that represents the data by a mixture of finite Gaussian probability density functions (PDF) [26] as

$$f(S^P, S^t | \theta_i) = \sum_{i=1}^{K} h_i \mathcal{N}(S^P, S^t | \mu_i, \Sigma_i) \tag{6}$$

in which

$$\mathcal{N}(S^P, S^t | \mu_i, \Sigma_i)$$
$$= \frac{1}{\sqrt{(2\pi)^3 |\Sigma_i|}} e^{-\frac{1}{2}\left(([S^P;S^t] - \mu_i)^T \Sigma_i^{-1}\left(([S^P;S^t] - \mu_i)\right)\right)} \tag{7}$$

$$\mu_i = \begin{bmatrix} \mu_i^P \\ \mu_i^t \end{bmatrix}, \Sigma_i = \begin{bmatrix} \Sigma_i^P & \Sigma_i^{Pt} \\ \Sigma_i^{tP} & \Sigma_i^t \end{bmatrix} \tag{8}$$

where $\mathcal{N}$ represents the joint 3-dimensional normal probability density function (PDF). K is the number of Gaussian mixture models. $\theta_i = \{h_i \in R^3, \ \mu_i \in R^3, \ \Sigma_i \in R^{3 \times 3}\}_{i=1}^K$, denotes the prior weight, the mean value and the covariance matrix for each of Gaussian mixture components, respectively. The Expectation-Maximization (EM) algorithm [27] is used to iteratively train the GMM model (θ_i) on total dataset (D), which is subject to the following constraint:

$$\sum_{i=1}^{K} h_i = 1, \forall i; \ 0 < h_i < 1 \tag{9}$$

The obtained GMM models should be customized to be utilized for the trajectory following task of pick and place considered in this paper. The average demonstrated position in a given time is needed for feeding to the controller later in robotic-assistance phase. This conditional probability is achieved using Gaussian Mixture Regression (GMR) [22] as

$$f(S^P | S^t = t) = \sum_{i=1}^{K} \omega_i \mathcal{N}\left(S^P \middle| \widehat{\mu_i^P}, \widehat{\Sigma_i^P}\right) \tag{10}$$

$$\mathcal{N}\left(S^P \middle| \widehat{\mu_i^P}, \widehat{\Sigma_i^P}\right) =$$
$$\frac{1}{\sqrt{(2\pi)^2 \left| \widehat{\Sigma_i^P} \right|}} e^{-\frac{1}{2}\left((s^P - \widehat{\mu_i^P})^T \widehat{\Sigma_i^P}^{-1}\left((s^P - \widehat{\mu_i^P})\right)\right)} \tag{11}$$

where $\widehat{\mu^P}, \widehat{\Sigma^P}$ are the expected mean and covariance matrix of the ith conditional probability as

$$\widehat{\mu_i^P} = \mu_i^P + \Sigma_i^{Pt}(\Sigma_i^t)^{-1}(S^t - \mu_i^t) \in R^2 \tag{12}$$

$$\widehat{\Sigma_i^P} = \Sigma_i^t + \Sigma_i^{Pt}(\Sigma_i^t)^{-1}\Sigma_i^{tP} \in R^{2\times2}. \tag{13}$$

The probability that S^t is in the ith Gaussian distribution component (ω_i) is

$$\omega_i = P(i|S^t = t) = \frac{h_i \mathcal{N}(S^t|\mu_i^t,\Sigma_i^t)}{\sum_{l=1}^{K} h_l \mathcal{N}(S^t|\mu_i^t,\Sigma_i^t)} \tag{14}$$

now, the single Gaussian distribution of the conditional expectation of S^p, given $S^t = t$, can be approximated as

$$f(S^P|S^t = t) \approx \mathcal{N}(S^P|\widehat{\mu^P},\widehat{\Sigma^P}), \tag{15}$$

$$\widehat{\mu^P} = \sum_{i=1}^{K} \omega_i.\widehat{\mu_i^P}, \ \widehat{\Sigma^P} = \sum_{i=1}^{K} \omega_i^2.\widehat{\Sigma_i^P} \tag{16}$$

$\widehat{\mu^P}$ is the average position demonstrated during the cooperation of the child and the therapist at each time. Considering the orthonormal 2-dimensional Cartesian $X_1 - X_2$ coordinates, these vectors can be rewritten as

$$\widehat{\mu_t^p} = \begin{bmatrix} \widehat{\mu_t^{P_{X_1}}} \\ \widehat{\mu_t^{P_{X_2}}} \end{bmatrix}, \tag{17}$$

where the subscript t represents the time in which the $\widehat{\mu^p}$ is achieved. $\widehat{\mu_t^{P_{X_1}}} \in R$ and $\widehat{\mu_t^{P_{X_2}}} \in R$ denote the projection of $\widehat{\mu_t^P}$ along the X_1 and X_2 coordinates, respectively.

In summary, the demonstrated trajectory is modeled in the $X_1 - X_2 - t$ space via the GMM/GMR algorithms. For a given time, the expected 2-dimensional $X_1 - X_2$ statistical model for the demonstrated position is approximated via (15)-(16). Then, the expected average position in that time is calculated in each of X_1 and X_2 using (17), which will be later utilized in our proposed controller (Fig. 4).

(a)

(b)
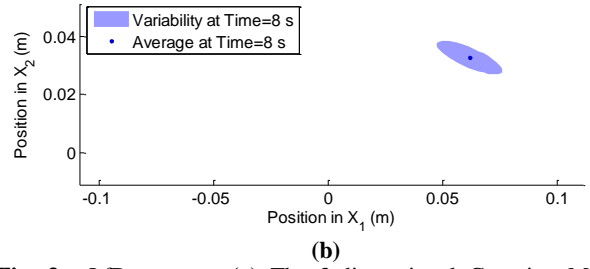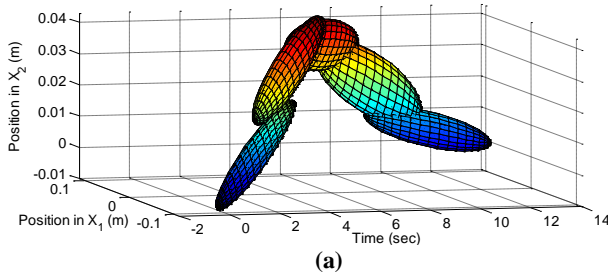
Fig. 3. LfD process: **(a)** The 3-dimensional Gaussian Mixture Models (GMM) capture the 3-dimensional $X_1 - X_2 - t$ dataset (D), and **(b)** The 2-dimentional $X_1 - X_2$ Gaussian probability density function (pdf) in a given time (t = 8s) resulting from GMR.

4. ROBOTIC ASSISTANCE PHASE

In this section, the aim is to propose a framework which utilizes the learnt average demonstrated position from the previous section so that the robot can take over the therapist's role and autonomously assist the child to follow the desired point-to-point trajectory in the pick and place task. In this framework, two desired virtual impedance models are defined in the master robot. These impedance models control the interaction dynamic of the master robot around the average demonstrated trajectory $(\widehat{\mu_t^P})$ in tangential and normal directions. Then, the slave robot, which is in contact with task environment, follows the master position through a unilateral teleportation system so that the child can perform the task on his/her own.

4.1. Master robot's tangential-normal impedance controller

The objective is to design a framework so that the master robot imitates the therapist's demonstrated performance and provides assistance to the child to follow the average demonstrated position trajectory from point A to point B. Depending on the task and the child, it may be desirable for the therapist to provide different levels of assistance/resistance in directions that are tangential/normal to the trajectory's direction. For this purpose, a tangential-normal coordinate T-N in each time is defined by setting the average demonstrated position at the current time $(\widehat{\mu_t^P})$ as the origin of the new T-N coordinate. The rotation of the T-N frame can be computed via differentiating the average position trajectory $(\widehat{\mu_t^P})$ as

$$\theta_{T,t} = Arctan\left(\left(\widehat{\mu_t^{P_{X_2}}} - \widehat{\mu_{t-\Delta t}^{P_{X_2}}}\right)\bigg/\left(\widehat{\mu_t^{P_{X_1}}} - \widehat{\mu_{t-\Delta t}^{P_{X_1}}}\right)\right) \tag{18}$$

$$R_t = \begin{bmatrix} \cos(\theta_{T,t}) & \sin(\theta_{T,t}) \\ -\sin(\theta_{T,t}) & \cos(\theta_{T,t}) \end{bmatrix} \tag{19}$$

$$H_t = \begin{bmatrix} & R_t & & -\widehat{\mu_t^{P_{X_1}}} \\ & & & -\widehat{\mu_t^{P_{X_2}}} \\ 0 & 0 & 1 \end{bmatrix}_{3\times3} \tag{20}$$

where $\theta_{T,t} \in [-\pi \ \pi]$ denotes the angle between the T-N and $X_1 - X_2$ Cartesian coordinates in a given time ($S^t = t$), calculated by four-quadrant inverse tangent. Δt represents the sampling period. R_t and H_t express the rotation and homogeneous transformation matrix [28], which maps each interaction force and position vector from X_1-X_2 to T-N coordinate at a given time (t) as

$$\begin{bmatrix} F_T \\ F_N \end{bmatrix} = R_t \begin{bmatrix} F_{X_1} \\ F_{X_2} \end{bmatrix}, \tag{21}$$

$$\begin{bmatrix} x_T \\ x_N \\ 1 \end{bmatrix} = H_t \begin{bmatrix} x_{X_1} \\ x_{X_2} \\ 1 \end{bmatrix} \tag{22}$$

In the next step, at a given time, two virtual impedance model are defined in directions tangential and normal to the average demonstrated trajectory. This models indicates the desired linear interaction dynamic between the master robot and the target trajectory in T-N Cartesian space (Fig. 4) as

$$m_T \ddot{\tilde{x}}_T + c_T \dot{\tilde{x}}_T + k_T \tilde{x}_T = -F_{ch,T} \tag{23}$$

$$m_N \ddot{\tilde{x}}_N + c_N \dot{\tilde{x}}_N + k_N \tilde{x}_N = -F_{ch,N} \tag{24}$$

where $\{m_T, c_T, k_T\} \in R^+$ and $\{m_N, c_N, k_N\} \in R^+$ refer to the desired virtual mass, damping and stiffness parameters in the tangential and normal directions, respectively. $\tilde{x}_T = x_{des,T} - x_{dem,T}$ and $\tilde{x}_N = x_{des,N} - x_{dem,N}$ indicate the difference between the desired robot position $\{x_{des,T}, x_{des,N}\} \in R$ and the demonstrated trajectory at a given time $\{x_{dem,T}, x_{dem,N}\} \in R$ as transformed to the T-N frame, respectively. $F_{ch,T}$ and $F_{ch,N} \in R$ denote the interaction force between the child and the master robot in T-N coordinates, which are found as

$$\begin{bmatrix} F_{ch,T} \\ F_{ch,N} \end{bmatrix} = R_t \begin{bmatrix} F_{ch,X_1} \\ F_{ch,X_2} \end{bmatrix} \tag{25}$$

and, the average demonstrated trajectory T-N coordinate is

$$\begin{bmatrix} x_{dem,T} \\ x_{dem,N} \\ 1 \end{bmatrix} = H_t \begin{bmatrix} \widehat{\mu_t^{P_{X_1}}} \\ \widehat{\mu_t^{P_{X_2}}} \\ 1 \end{bmatrix} = \begin{bmatrix} 0 \\ 0 \\ 1 \end{bmatrix} \tag{26}$$

Equivalently, $\dot{\tilde{x}}_T$, $\ddot{\tilde{x}}_T$, $\dot{\tilde{x}}_R$ and $\ddot{\tilde{x}}_R$ are

$$\begin{bmatrix} \dot{\tilde{x}}_T \\ \dot{\tilde{x}}_N \end{bmatrix} = \begin{bmatrix} \dot{x}_{des,T} \\ \dot{x}_{des,N} \end{bmatrix} \in R^2 \tag{27}$$

$$\begin{bmatrix} \ddot{\tilde{x}}_T \\ \ddot{\tilde{x}}_N \end{bmatrix} = \begin{bmatrix} \ddot{x}_{des,T} \\ \ddot{x}_{des,N} \end{bmatrix} \in R^2 \tag{28}$$

In Fig. 4, the red and green orthogonal axes represent the T-N and $X_1 - X_2$ Cartesian coordinates respectively. The T-N origin is on the average demonstrated trajectory at a given time which acts as a moving target in this controller ($\widehat{\mu_t^p}$). In the first step, the child's applied force on the master (F_{ch}) is projected along T-N coordinates by (R_t) and then exerted to their corresponding virtual mass-damper-spring models that are connected to the virtual moving target ($\widehat{\mu_t^p}$). These forces cause a deviation with respect to the moving target and find the desired master robot position in each of tangential/normal directions ($x_{des,T}, x_{des,N}$), so that the master robot get connected to the desired virtual moving target via virtual impedance models. These desired positions are then map back to $X_1 - X_2$ coordinate (29) for the master robot to be followed. Accordingly, the child feels as if connected to a moving target ($\widehat{\mu_t^p}$) via virtual mass-damper-spring impedance models in each of tangential and normal directions (Fig. 4).
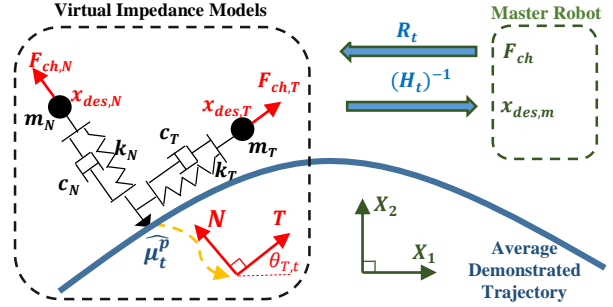
Fig. 4. The proposed virtual Tangential-Normal impedance controller.

Therefore, the master robot not only follows the average demonstrated position, but also provides an adjustable level of freedom for the child to deviate from this trajectory in each direction. The larger the desired impedance parameters, the less the child's freedom to deviate from the expected trajectory.

$$\begin{bmatrix} x_{des,X_1} \\ x_{des,X_2} \\ 1 \end{bmatrix} = H_t^{-1} \begin{bmatrix} x_{des,X_T} \\ x_{des,X_N} \\ 1 \end{bmatrix} \tag{29}$$

4.2 Unilateral teleoperation control

A unilateral teleoperation system (Fig. 5) is used, where the master position is transmitted to the slave side to be used as the desired position for slave:

$$x_{des,s} = x_m. \tag{30}$$

Here, $x_{des,s} \in R^2$ denotes the desired position for slave robot. And, $x_m \in R^2$ expresses the master robot position transmitted from master side. A PID controller is utilized, so that the master and slave robots follow their desired positions.
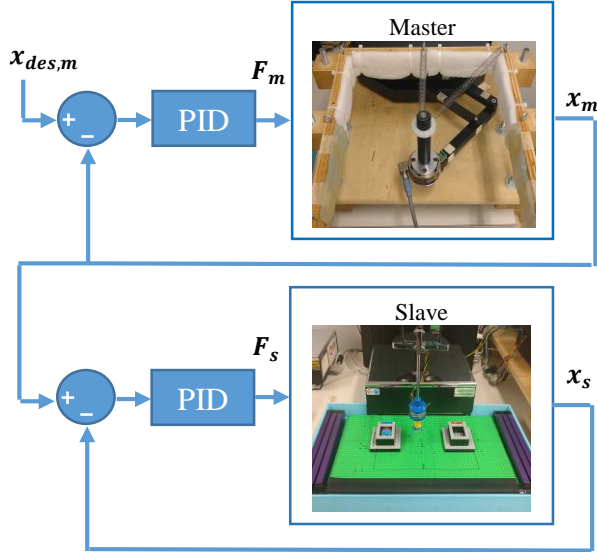
Fig. 5. Unilateral teleoperation system. The slave robot (in play environment) follows the position of master robot (child) that is connected to the virtual T-N impedance models.

6. EXPERIMENTS AND DISCUSSION

The proposed ANN framework using LfD is experimentally tested using a Quanser Rehab robot (Quanser Consulting Inc., Markham, Canada) as the master (Fig. 6a) and a Phantom Premium robot (Geomagic Inc., Wilmington, USA) as the slave (Fig. 6a). Both of the therapist demonstration and robotic assistance phases are implemented with a sampling time of 1 $m$sec using the QUARC real-time control software (Quanser Consulting Inc., Markham, Canada).

A game is designed for the child such that he/she moves the slave robot through a teleoperation system, in order to pick a token from box A in a 2D play environment and put it in box B (see Fig. 6). A coil is mounted on the slave end-effector and charged with electrical current when the robot reaches the box A for picking the metal token. This coil is discharged when the slave end-effector reach the box B for placing the token in this box.
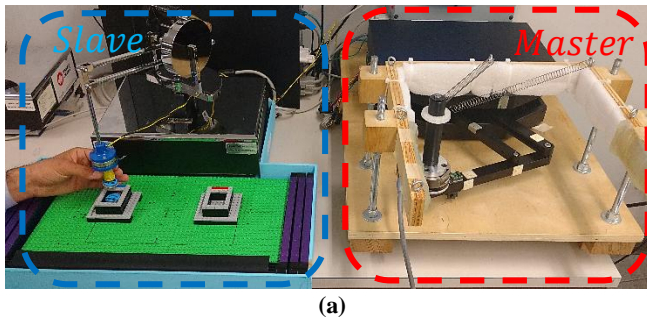
(a)
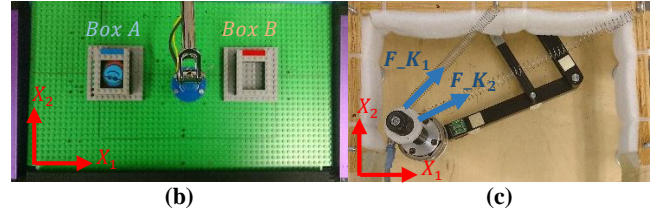
Fig. 6. The experimental set up: **(a)** Quanser Rehab robot (Master) and Phantom Premium robot (Slave) in the teleoperation system, **(b)** the game environment, where the task is to pick tokens from box A and place them in box B, and **(c)** the spring array (K_1, K_2), modeling the child with disability in the master robot side.

6.1 Demonstration Phase

In this experiment, the child is simulated as a spring array that is pulled to the box A location at the beginning of the experiment (Fig. 6.c). This array will produce 2D forces while reaching its' equilibrium point, which is not the box B's location. Therefore, the simulated CP child cannot move the master and consequently the slave to the box B location and accomplish the pick and place task, as shown in Fig. 7, if unassisted.
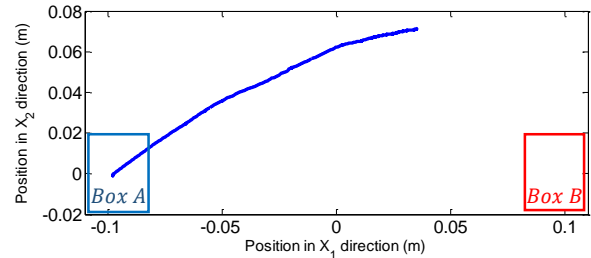
Fig. 7. The simulated CP child (spring array) trajectory without therapist/robotic assistance.

Accordingly, it is required that in the demonstration phase the therapist assists the child to correct the movement by applying assistive/resistive forces to the slave end-effector in the tangential/normal directions. This assistance is provided on an as-needed basis by considering the unique motion characteristic of the child. The obtained trajectories of the child and the therapist across 5 trials are shown in Fig. 8a. The GMM of these trajectories are shown in Fig. 8b. The average demonstrated trajectory and the corresponding variation manifold obtained from GMR are also illustrated in Fig. 8c.

(a)

6

(b)

(c)
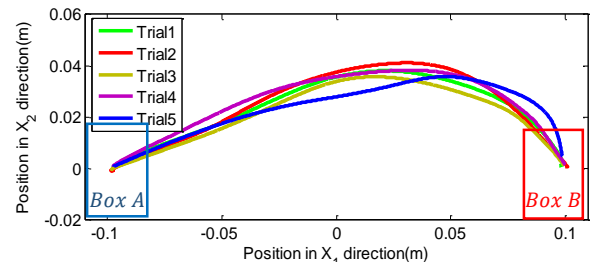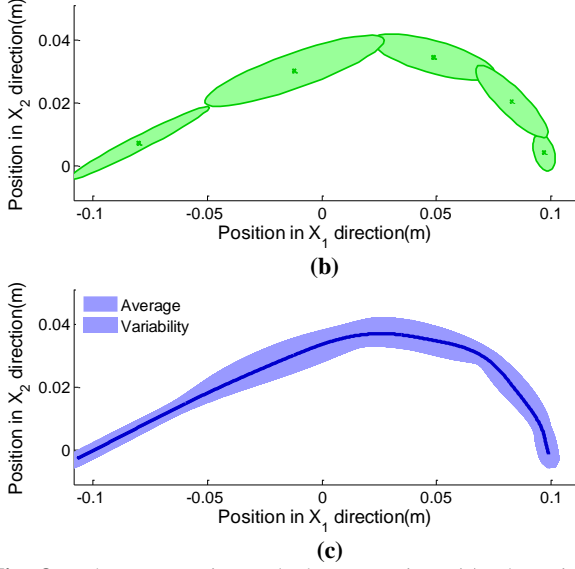
Fig. 8. The cooperative task demonstration: **(a)** Therapist-child mutual position, executing the pick and place task for 5 trials, **(b)** the projection of 3D GMM on the $X_1 - X_2$ Cartesian coordinates, **(c)** the average and variability of the demonstrated trajectories, resulting from GMR.

As seen in Fig. 8, the GMM and GMR models efficiently capture the average and variability of cooperative task execution. The therapist interaction force in Tangential and Normal directions for the trial number 4 is sketched in Fig. 9.

(a)

(b)
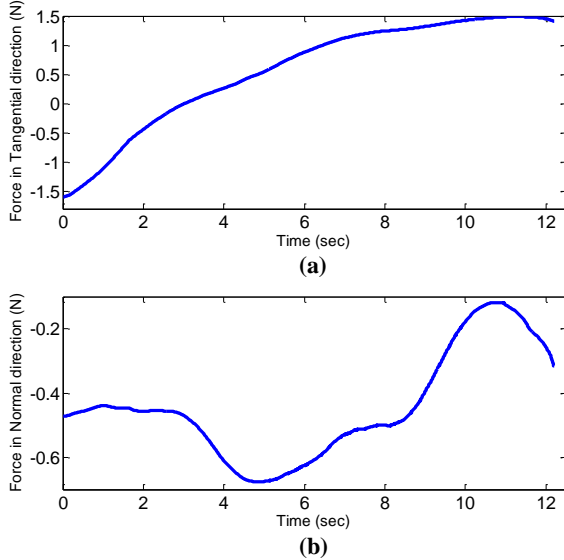
Fig. 9. Therapist-applied force in the task demonstration: **(a)** in Tangential direction, and **(b)** in Normal direction.

Based on the structure of utilized spring array, the simulated child will exert a force in the normal direction along the trajectory. Thus, the therapist applied force in opposite direction (Fig. 9b) to increase resistance in normal direction and bend the mutual trajectory toward box B, while preserving the curve-like motion characteristic of child (Fig.

7), in tangential direction. At first, the therapist applied force in negative direction to reduce the abrupt acceleration of the robots produced by spring array in Box A location (Fig. 9a). Then, the therapist has provided the positive force to assist the child to reach the destination.

6.2 Robotic Assistance Phase

The demonstrated average trajectory of the child-therapist cooperation in the previous phase are employed in this phase to perform the task in the absence of the therapist. The child deviation (in this phase) with respect to the demonstrated average trajectory (from the previous phase) is determined as a response to his/her interaction forces, using the proposed tangential-normal impedance models (23), (24). In order to evaluate the performance of the impedance model in terms of adjustment of the child's flexibility, different sets of impedance models are defined and listed in Table 1.

TABLE 1
Adjustment of tangential and normal impedance models for various set of parameters.

T < N	M	C	k	*ST*
Tangential (T)	$50\times ST$	$140\times ST$	$200\times ST$	{1,2,3}
Normal (N)	$100\times ST$	$280\times ST$	$400\times ST$	
N < T	**m**	**C**	**k**	*SN*
Tangential (T)	$100\times SN$	$280\times SN$	$400\times SN$	{1,2,3}
Normal (N)	$50\times SN$	$140\times SN$	$200\times SN$	

Impedance parameters are chosen to provide the robot with appropriate transient response to child's input forces and cancel the high frequency response, which corresponds to tremor in children with CP:

$$\xi = c/2\sqrt{m.k} = 0.7 \tag{31}$$

$$\omega_n = \sqrt{k/m} = 2 \tag{32}$$

Using these parameters in the virtual impedance models and applying the proposed impedance control strategy to follow the average demonstrated trajectory, the $X_1 - X_2$ trajectory of the slave robot (in the task environment) is as shown in Fig. 10.

(a)

7

(b)
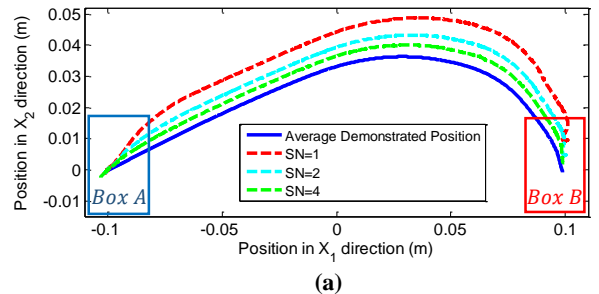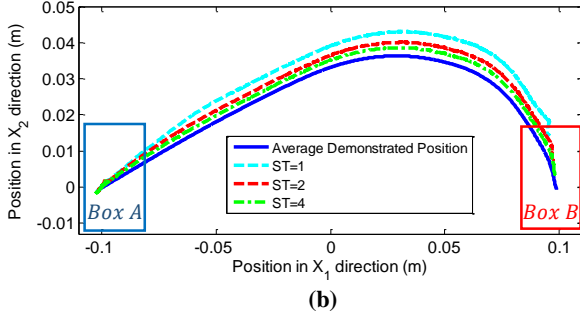
Fig. 10. Robotic assistance phase. Child's trajectory: **(a)** more flexibility (less resistance) in the normal direction, and **(b)** more flexibility (less assistance) in the tangential direction.

Impedance parameters adjust the trade-off between accuracy (more assistance/resistance) and flexibility (less assistance/resistance) in each of tangential/normal directions. Movement in the tangential direction highly contributes to the task accomplishment as the child is moving along the average demonstrated trajectory to reach the destination (box B). So, it is desirable to provide the child with more flexibility (less assistance) in the tangential direction to ensure his/her motivation and participation in task execution. However, the child's ability to move along the average trajectory should be taken into consideration. As it is observed in Fig. 10b, choosing the impedance parameters by adjusting ST=1, the child is unable to reach the destination, because of inadequate assistance in the tangential direction.

Less resistance in the normal direction gives more freedom to the child for deviation in directions orthogonal to the tangential direction. The level of flexibility in the normal direction is limited by any spatial restriction in the task environment. In order to minimize this resistance and also, meet the required accuracy for task accomplishment, this parameter can be set according to the observed variability of demonstrated data in Fig. 8c.

Based on the above discussion, in this work, ST=2 has been selected for the assistance phase, which the adjusted impedance parameters not only provide more flexibility in the tangential direction, but also allows the child to have acceptable deviation in normal direction. The corresponding position deviations from the average trajectory in the T-N coordinates and also the applied interaction forces by the child in the T-N directions that generate these deviations, are sketched in Fig. 11.

(a)

(b)

(c)
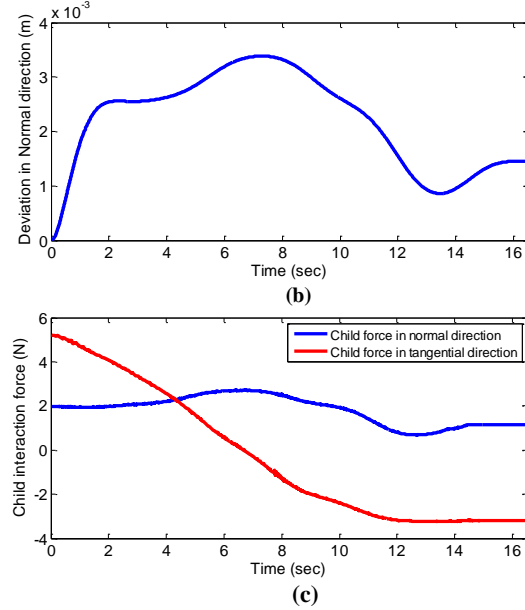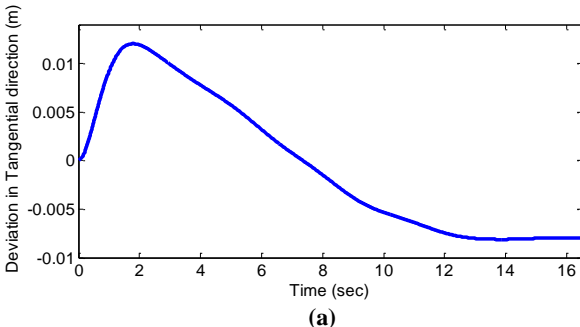
Fig. 11. Robotic assistance phase (ST=2): Child **(a)** deviation tangent to trajectory **(b)** deviation normal to the trajectory **(c)** interaction force in T-N coordinates.

7. CONCLUSION

In this work, a robotic-assistance-as-needed framework was proposed for children with Cerebral Palsy (CP) to perform 2D position following task, by tele-manipulating the slave robot in the play environment. In the first step (demonstration phase), the therapist interacted with the slave robot to assist and correct the child's movements. Using a learning from demonstration strategy, the Gaussian Mixture Model (GMM) and Gaussian Mixture Regression (GMR) techniques were utilized to approximate the average and variability of the demonstrated therapist-child trajectories.

Then, in the robotic assistance phase (without therapist intervention), the impedance/admittance control method was applied such that the master robot provides a desirable flexibility for the child during following the average trajectory. Different impedance characteristics were defined for the child deviation (flexibility) in normal and tangential directions with respect to the average trajectory. As small as needed impedance parameters were employed in the tangential direction to provide appropriate flexibility (assistance) for the child and execute the task. However, by increasing the impedance parameters corresponding to the normal direction, the child deviation from the desired trajectory decreases.

The validity of proposed framework was experimentally evaluated by using different sets of impedance parameters in tangential/normal impedance models. To have the same condition in different experiments, a spring array was designed for simulating the patient force on the master robot. In future works, the proposed strategy will be utilized for real children with CP to improve their ability and success rate in pick and place tasks on the play environment.

REFERENCES

[1] S. B. Koman LA, Shilt JS, "Cerebral palsy," *Lancet,* pp. 1619–1631, 2004.

[2] R. W. Armstrong, "Definition and classification of cerebral palsy," *Developmental Medicine andChild Neurology,* vol. 49, pp. 1-44, 2007.

[3] S. o. C. P. i. Europe, "Prevalence and characteristics of children with cerebral palsy in Europe," *Developmental Medicine and Child Neurology,* pp. 633–640, 2002.

[4] H. T. Paneth N, Korzeniewski S, "The descriptive epidemiology of cerebral palsy," *Clinics in Perinatology,* vol. 33, pp. 251-267, 2006.

[5] R. J. P. Suzann K. Campbell, Margo Orlin, *Physical Therapy for Children*, 4th ed., 2002.

[6] I. A.-R. Heidi Anttila, Jutta Suoranta, Marjukka Mäkelä, Antti Malmivaara, "Effectiveness of physical therapy interventions for children with cerebral palsy: A systematic review," *BMC Pediatrics* vol. 8, 2008.

[7] A. M. Ríos-Rincón, K. Adams, J. Magill-Evans, and A. Cook, "Playfulness in Children with Limited Motor Abilities When Using a Robot," *Physical & Occupational Therapy In Pediatrics,* vol. 36, pp. 232-246, 2016/07/02 2016.

[8] T. Klein, G. J. Gelderblom, L. d. Witte, and S. Vanstipelen, "Evaluation of short term effects of the IROMEC robotic toy for children with developmental disabilities," in *2011 IEEE International Conference on Rehabilitation Robotics*, 2011, pp. 1-5.

[9] K. H. Hogan N1, Rohrer B, Palazzolo JJ, Dipietro L, Fasoli SE, Stein J, Hughes R, Frontera WR, Lynch D, Volpe BT., "Motions or muscles? some behavioral factors underlying robotic assistance of motor recovery," *Journal of rehabilitation research and development* vol. 43(5), pp. 605-618, 2006.

[10] A. V. Dowling, O. Barzilay, Y. Lombrozo, and A. Wolf, "An adaptive home-use robotic rehabilitation system for the upper body," *IEEE Journal of Translational Engineering in Health and Medicine,* vol. 2, pp. 1-10, 2014.

[11] H. I. Krebs, J. J. Palazzolo, L. Dipietro, M. Ferraro, J. Krol, K. Rannekleiv*, et al.*, "Rehabilitation Robotics: Performance-Based Progressive Robot-Assisted Therapy," *Autonomous Robots,* vol. 15, pp. 7-20, 2003.

[12] M. Tavakoli, A. Aziminejad, R. V. Patel, and M. Moallem, "High-Fidelity Bilateral Teleoperation Systems and the Effect of Multimodal Haptics," *IEEE Transactions on Systems, Man, and Cybernetics, Part B (Cybernetics),* vol. 37, pp. 1512-1528, 2007.

[13] G. V. A. G. A. Perera and A. M. H. S. Abeykoon, "Review on bilateral teleoperation with force, position, power and impedance scaling," in *7th International Conference on Information and Automation for Sustainability*, 2014, pp. 1-7.

[14] D. A. Lawrence, "Stability and transparency in bilateral teleoperation," in *Decision and Control, 1992., Proceedings of the 31st IEEE Conference on*, 1992, pp. 2649-2655 vol.3.

[15] M. Sharifi, S. Behzadipour, and H. Salarieh, "Nonlinear Bilateral Adaptive Impedance Control With Applications in Telesurgery and Telerehabilitation," *Journal of Dynamic Systems, Measurement, and Control,* vol. 138, pp. 111010 (16 pages), 2016.

[16] L. Marchal-Crespo and D. J. Reinkensmeyer, "Review of control strategies for robotic movement training after neurologic injury," *Journal of NeuroEngineering and Rehabilitation,* vol. 6, pp. 20-20, 2009.

[17] N. Hogan, "Impedance Control: An Approach to Manipulation," in *American Control Conference, 1984*, 1984, pp. 304-313.

[18] M. Sharifi, S. Behzadipour, and G. Vossoughi, "Nonlinear model reference adaptive impedance control for human–robot interactions," *Control Engineering Practice,* vol. 32, pp. 9-27, 2014.

[19] Y. Mao and S. K. Agrawal, "Design of a Cable-Driven Arm Exoskeleton (CAREX) for Neural Rehabilitation," *IEEE Transactions on Robotics,* vol. 28, pp. 922-931, 2012.

[20] M. Sharifi, S. Behzadipour, and G. R. Vossoughi, "Model reference adaptive impedance control of rehabilitation robots in operational space," in *2012 4th IEEE RAS & EMBS International Conference on Biomedical Robotics and Biomechatronics (BioRob)*, 2012, pp. 1698-1703.

[21] B. Ding, Q. Ai, Q. Liu, and W. Meng, "Path Control of a Rehabilitation Robot Using Virtual Tunnel and Adaptive Impedance Controller," in *Computational Intelligence and Design (ISCID), 2014 Seventh International Symposium on*, 2014, pp. 158-161.

[22] M. Maaref, A. Rezazadeh, K. Shamaei, and M. Tavakoli, "A Gaussian Mixture Framework for Co-Operative Rehabilitation Therapy in Assistive Impedance-Based Tasks," *IEEE Journal of Selected Topics in Signal Processing,* vol. 10, pp. 904-913, 2016.

[23] M. Maaref, A. Rezazadeh, K. Shamaei, R. Ocampo, and T. Mahdi, "A Bicycle Cranking Model for Assist-as-Needed Robotic Rehabilitation Therapy Using Learning From Demonstration," *IEEE Robotics and Automation Letters,* vol. 1, pp. 653-660, 2016.

[24] M. Hersch, F. Guenter, S. Calinon, and A. Billard, "Dynamical System Modulation for Robot Learning via Kinesthetic Demonstrations," *IEEE Transactions on Robotics,* vol. 24, pp. 1463-1467, 2008.

[25] L. W. Slotine JJE, *Applied nonlinear control*, 1991.

[26] S. Calinon, F. Guenter, and A. Billard, "On learning the statistical representation of a task and generalizing it to various contexts," in *Proceedings 2006 IEEE International Conference on Robotics and Automation, 2006. ICRA 2006.*, 2006, pp. 2978-2983.

[27] T. K. Moon, "The expectation-maximization algorithm," *IEEE Signal Processing Magazine,* vol. 13, pp. 47-60, 1996.

[28] J. J. Craig, *Introduction to Robotics: Mechanics and Control* 3rd ed., 1989.